Predicting Drying in Multiple-Zone Ovens

Sacide Alsoy*

Department of Chemical Engineering, Izmir Institute of Technology, Gaziosmanpasa Bulvari, No. 16 35230 Cankaya-Izmir, Turkey

In the coating industry, the drying of solvent-coated polymeric films takes place in convected heated dryers, which usually consist of a series of zones. The operating conditions of airflow, solvent partial pressure(s), and temperature at the entrance of each zone are chosen to minimize the drying time while maintaining an acceptable product quality. In this work, the drying behavior of polymer solutions in such oven configurations is predicted from binary and multicomponent drying models. Both models involve coupled heat- and mass-transfer equations that describe the changes in the concentration of each solvent, the temperature, and the thickness of the film throughout the drying. The model equations become highly nonlinear because of the strong and complicated concentration and temperature dependencies of the thermodynamic and transport properties of polymer solutions. These nonlinear equations are solved numerically using the finite difference approximation. The solutions show that multiple-zone ovens can be used to eliminate bubble formation and to minimize the residual solvent content by controlling the operating conditions individually or simultaneously.

Introduction

Many thin coated polymeric products such as photographic films, synthetic fibers, and adhesives are produced by casting a continuous single layer of polymer solution or multiple distinct solution layers onto a moving substrate and forming the final product as these layers are dried in an oven with forced air convection. Usually, the drying step is considered to be responsible for the structure and properties of the final product, as it is the last step in the process. Some problems such as phase separations, bubble formation, and various kinds of stress-related defects are observed when drying is not adequately controlled.[1,2] Therefore, accurate modeling of this process becomes crucial for process design, optimization, product scale-up, and defect analysis.

The drying of solvent-coated polymer films involves simultaneous heat and mass transfer within the shrinking film controlled by the complex thermodynamic and transport properties of polymer solutions. Similar transport processes also take place in the gas phase. Drying characteristics are initially determined by external conditions such as the heat- and mass-transfer coefficients, the gas-phase temperature and velocity, and the partial pressure and activity of each solvent. This period is short compared to the total drying time, and usually, the overall process is controlled by diffusion in the polymer phase.[3] This is because of the unusual and complex transport and thermodynamic properties of polymer solutions. In mixtures of low-molecular-weight molecules, molecular migration is typically a weak function of temperature and concentration, whereas in polymeric systems, diffusional transport can be significantly enhanced or diminished by varying either condition, as shown by Vrentas and Duda.[4−6] During the drying of polymer solutions, the diffusivities decrease by several orders of magnitude as the solvent concentration decreases, especially within the layer of steeply falling concentration near the free surface.[2,3] This phenomenon is referred to as "skinning", which is defined as the development of a layer at the surface of the coating whose characteristics differ significantly from the material deeper in the coating. The drying theories used in this article predict when this type of skinning might occur. Skin formation is one of the commonly reported problems in the coating industry. Even though creating a dense microstructure near the surface is a desirable phenomenon in membrane production, skinning is not wanted in coating processes because it can lead to stress development and deformation or cracking of the surface of the coating; decreased drying rates; the formation and retention of bubbles within the coating; and nonuniform microstructure, chemical composition, and properties throughout the coating.[1]

The choice of oven type and drying conditions strongly influences skin formation and other coating defects or problems associated with drying, as well as the total residual solvent level in the final coating. For example, an air temperature that is too high can cause bubble formation or degradation of coating properties, whereas air velocities that are too high can disturb the coating and cause defects that appear as bands or as mottle.[8] The effect of oven design on drying rate and bubble formation was predicted by Cairncross et al.[2] According to their results, multiple-zone ovens can help remove solvents faster while achieving better product quality. These facts indicate the importance of a detailed model to use as a tool for optimizing both the design and the process conditions.

Many models exist in the literature for predicting the drying behavior of binary polymer solutions.[2,9−16] However, multicomponent drying models are limited because of the lack of diffusion data and the difficulty in handling complex transport equations.[7,13] Previously, the binary drying model developed by Vrentas and Vrentas[15] and the multicomponent drying model developed by Alsoy and Duda[7] were successfully used to predict the drying rate of polymer−solvent coatings in single-zone ovens. This article discusses the relevance

* Tel.: +90 232 498 6273. Fax: +90 232 498 6355. E-mail: sacide@likya.iyte.edu.tr.

10.1021/ie000751+ CCC: $20.00
Published on Web 05/15/2001

of these models in predicting the drying characteristics of polymer solutions in multiple-zone ovens. The models are applied to an acetone-based cellulose acetate coating and a toluene−tetrahydrofuran-based polystyrene coating. The validity of the binary drying model is confirmed by comparing predictions with the drying data collected for the polyvinyl acetate−toluene system.

Theory

The following theory is applicable to predictions of the drying behavior of nonreactive coatings that consist of a polymer dissolved in multiple solvents. In this theory, mass transport is assumed to be one-dimensional, and the generalized Fick's law is used to describe the difffusive flux equations for the multicomponent system. Furthermore, it is assumed that the partial specific volume of each component in the mixture is constant. Then, the species continuity equation is given by the equation

$$\frac{\partial \rho_i^{\mathrm{p}}}{\partial t} = \frac{\partial}{\partial x}\left(\sum_{j=1}^{N-1} D_{ij}^{\mathrm{p}} \frac{\partial \rho_j^{\mathrm{p}}}{\partial x}\right) \tag{1}$$

where ρ_i^{p} is the mass density of species i and D_{ii}^{p} and D_{ij}^{p} are the mutual diffusion coefficients in the multicomponent mixture called as main and cross diffusion coefficients, respectively. The heat transport through drying is approximated by a lumped-parameter approach. Thus, the temperature is uniform across any section from the top of the coating to the bottom of the web. This is a reasonable assumption because, under most drying conditions, the resistance to heat transfer is much greater in the gas phase than in the polymer or substrate layer. The validity of the approximation of neglecting temperature gradients in the polymer and substrate layers is confirmed by the detailed analysis of Yapel.[13] The time dependence of the temperature is then given by

$$\frac{\mathrm{d}T}{\mathrm{d}t} = -\left[\frac{h^{\mathrm{G}}(T - T^{\mathrm{G}}) + \sum_{i=1}^{N-1} k_i^{\mathrm{G}} \Delta \hat{H}_{vi}(P_{ii}^{\mathrm{G}} - P_{i\mathrm{b}}^{\mathrm{G}}) + h^{\mathrm{g}}(T - T^{\mathrm{g}})}{\rho^{\mathrm{p}} \hat{C}_{\mathrm{p}}^{\mathrm{p}} X(t) + \rho^{\mathrm{s}} \hat{C}_{\mathrm{p}}^{\mathrm{s}} H}\right] \tag{2}$$

where T is the temperature of the coating and substrate and T^{G}, T^{g}, h^{G}, and h^{g} are the temperatures and heat-transfer coefficients of the upper- and lower-side gas streams, respectively. Also, k_i^{G} is the mass-transfer coefficient, $\Delta \hat{H}_{vi}$ is the heat of vaporization, P_{ii}^{G} is the partial pressure at the gas−polymer film interface, and $P_{i\mathrm{b}}^{\mathrm{G}}$ is the bulk pressure of component i. ρ^{p} and ρ^{s} are the densities and $\hat{C}_{\mathrm{p}}^{\mathrm{p}}$ and $\hat{C}_{\mathrm{p}}^{\mathrm{s}}$ are the specific heats of the polymer film and substrate, respectively. As the solvents diffuse through the slab and evaporate from the polymer film−air interface, the thickness of the film decreases. The time dependence of the film thickness is obtained from a jump mass balance for the polymer and is given by

$$\frac{\mathrm{d}X}{\mathrm{d}t} = -\left[\frac{\sum_{i=1}^{N-1} J_i^{\mathrm{p}\neq} \hat{V}_i^{\mathrm{p}}}{1 - \sum_{i=1}^{N-1} \rho_i^{\mathrm{p}} \hat{V}_i^{\mathrm{p}}}\right] \tag{3}$$

where $J_i^{\mathrm{p}\neq}$ is the diffusive flux based on the volume-average velocity and $\hat{V}_i^{\mathrm{p}}$ is the specific volume of component i in the polymer phase. To solve these equations, required boundary conditions can be written as

$$x = 0: \quad \frac{\partial \rho_i^{\mathrm{p}}}{\partial x} = 0 \tag{4}$$

$$x = X(t): \quad -\left[\sum_{j=1}^{N-1} D_{ij}^{\mathrm{p}} \frac{\partial \rho_j^{\mathrm{p}}}{\partial x}\right] - \rho_i^{\mathrm{p}} \frac{\mathrm{d}X}{\mathrm{d}t} = k_i^{\mathrm{G}}(P_{ii}^{\mathrm{G}} - P_{i\mathrm{b}}^{\mathrm{G}}) \tag{5}$$

Equation 4 expresses the lack of mass flux into the substrate. In other words, it is assumed that the substrate is impermeable to the components in the coating mixture. Equation 5, though somewhat complicated in appearance, states the continuity of mass fluxes at the interface of the coating with the surrounding air. The basic assumption utilized in deriving eq 5 is that there is no accumulation at the interface. The condition is complicated by the motion of the interface as the film thins during drying. Finally, initial conditions are given by the equations

$$\rho_i^{\mathrm{p}}(0,x) = \rho_{i\mathrm{o}}^{\mathrm{p}} \tag{6}$$

$$X(0) = L \qquad T(0) = T_{\mathrm{o}} \tag{7}$$

where $\rho_{i\mathrm{o}}^{\mathrm{p}}$ is the initial mass density of component i in the polymer film, T_{o} is the initial temperature of the polymer film and substrate, and L is the initial thickness of the polymer film. The model equations presented above are highly nonlinear and can be solved only by numerical techniques. To facilitate numerical treatment of the moving interface, a coordinate transformation was used. Equations updated according to the coordinate transformation were solved using the finite difference method with a variable grid size. The details of the coordinate transformation and numerical solution procedure can be found elsewhere.[3]

Results and Discussion

The drying characteristics predicted by the theory presented here are initially determined by external conditions in the drying atmosphere and afterward by the diffusion of solvents within the solution. The duration of the initial drying period depends on the heat- and mass-transfer coefficients, the heat of evaporation, the vapor pressures of the solvents in the bulk and at the polymer−gas interface, and the activity of each solvent. When the concentration of solvents at the surface become very low, the falling rate period starts, and drying is controlled by diffusional resistance within the film. For polymer solutions, the overall drying rate is usually controlled by falling rate period. Consequently, the key issue in accurately modeling the process is the prediction of the diffusivities in polymer−solvent solution. For a binary system, a single mutual-diffusion coefficient is required to describe the diffusive

Table 1. Free-Volume Parameters Used in Diffusivity Correlations

parameter		PVAC toluene	PS THF	PS toluene	CA acetone
D_o	cm²/s	4.82×10^{-4}	14.4×10^{-4}	4.82×10^{-4}	14.3×10^{-4}
E	J/mol	0	0	0	0
K_{11}/γ	cm³/(g K)	14.5×10^{-4}	7.5×10^{-4}	14.5×10^{-4}	9.83×10^{-4}
K_{12}/γ	cm³/(g K)	4.33×10^{-4}	5.82×10^{-4}	5.82×10^{-4}	4.35×10^{-4}
$K_{21} - T_{g1}$	K	−86.32	10.45	−86.32	−12.12
$K_{22} - T_{g2}$	K	−258.2	−327	−327	−240
$\hat{V}_1^*$	cm³/g	0.917	0.899	0.917	0.943
$\hat{V}_{2S}^*\xi$	cm³/g	0.597	0.383	0.493	0.615
χ		0.393	0.34	0.354	0.5

Table 2. Parameters for the Cellulose Acetate−Acetone System

initial conditions	
temperature	298 K
coating thickness	0.00577 cm
initial composition of solvent	0.7 g/cm³
substrate parameters	
heat capacity	1.25J/g K
density	1.37 g/cm³
base thickness	0.003556 cm
coating parameters	
heat capacity	2.1 J/g K
density of polymer	1.31 g/cm³
heat of vaporization of solvent	552 J/g
operating conditions	
base-side heat-transfer coefficient	6×10^{-4} W/(cm² K)
coat-side heat-transfer coefficient	6×10^{-4} W/(cm² K)
bottom air supply temperature	343 K
top air supply temperature	343 K
mass-transfer coefficient of solvent	8×10^{-10} s/cm
mole fraction of solvent in the gas phase	0

flux within the film. The formalism proposed by Vrentas and Duda has been successfully used to calculate binary diffusion coefficients.[17−19] Theoretically, diffusion in a ternary system is described by four diffusion coefficients. The prediction of these diffusivities from the most general form of the multicomponent diffusion theory requires knowledge of the friction coefficients that provide a link between the self- and mutual-diffusion coefficients in the multicomponent mixtures.[20,21] Unfortunately, no experimental measurements are available for these coefficients or for multicomponent diffusivites in polymer−solvent mixtures. Therefore, practical use of the generalized multicomponent diffusion theory is not currently possible. To overcome this problem, a few useful friction-based theories have recently been suggested that all stem from Bearman's formalism through assumptions regarding the individual friction coefficients.[7,22] These theories combine self-diffusion coefficients with thermodynamic factors as in the formulation of binary diffusion coefficients. In this work, the theory proposed by Alsoy and Duda was used to predict ternary diffusion coefficients.[7] Self-diffusion coefficients and chemical potentials required in this formalism were calculated from the Vrentas−Duda free-volume theory and the Flory−Huggins theory, respectively.[23−25] In the following paragraphs, the results of first binary and then multicomponent drying predictions are shown.

(a) Cellulose Acetate−Acetone System. The model was first applied to an acetone-based cellulose acetate (CA) coating. The free-volume parameters and other input data used in the simulations are given in Tables 1 and 2, respectively. The acetone free-volume parameters and the Flory−Huggins interaction parameter are available in the literature, and the cellulose acetate free-volume parameters were regressed from experimental

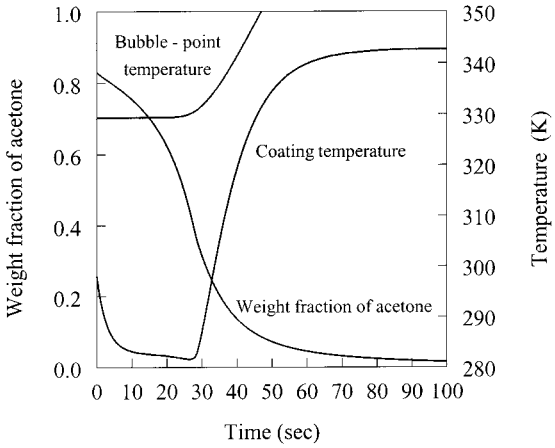

Figure 1. Prediction of the drying of a cellulose acetate−acetone coating in a single-zone oven under low airflow. The oven temperature is 70 °C, and the heat-transfer coefficients are both 6×10^{-4} W/(cm² K).

measurements of self-diffusion coefficients.[26−28] The prediction results are plotted in Figures 1−6. Figure 1 shows the weight fraction of acetone and the temperature of the coating and substrate as the sample passes through a single drying zone. Most of the acetone is removed in the first 50 s, indicating that the drying rate is highest at the beginning and then slows because of the increasing diffusional resistance to mass transfer within the film. A minimum in the coating temperature is observed because evaporative cooling due to the latent heat of vaporization of the solvent initially dominates. The temperature remains almost constant between 10 and 30 s. Within this period, the latent energy lost because of evaporation is just replenished by energy transfer to the solution by the hot air blown from the top and backside of the coating. After 30 s of drying, convective heating of the polymer film and substrate becomes dominant, and the temperature of the system approaches the oven temperature. Figure 1 also shows the bubble-point temperature as a function of time. The bubble-point temperature is defined as the temperature at which the local equilibrium solvent partial pressure equals atmospheric pressure. To calculate the partial pressure of acetone, its activity in the solution was predicted by Flory−Huggins theory and the vapor pressure, P_i^o, was estimated from the correlation[29]

$$\ln \frac{P_i^o}{P_c} = \frac{1}{(1-x)}[Ax + Bx^{1.5} + Cx^3 + Dx^6] \qquad (8)$$

$$x = 1 - \frac{T}{T_c} \qquad (9)$$

where P_c and T_c are the critical pressure and temperature of the solvent, respectively, and A, B, C, and D are constants. The partial pressure of the solvent varies throughout the coating because it is a function of both the solvent concentration and the temperature. It rapidly drops to near zero at the surface of the coating because of diffusional resistance and remains high at the substrate of the coating. Consequently, bubble formation starts from the substrate−coating interface, and so, the prediction of the bubble-point temperature was only shown at this point. In addition to solvent boiling, bubbles can also be introduced into the coating process through impurities such as dissolved gases

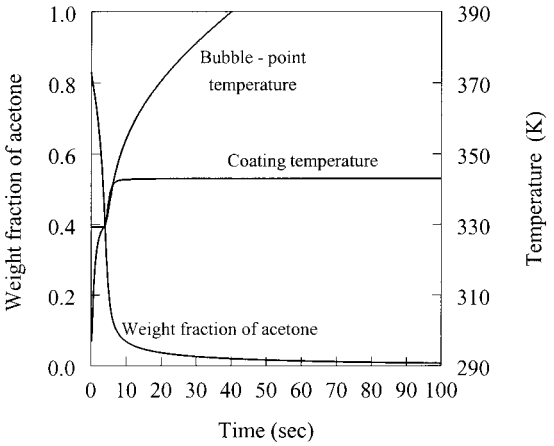

Figure 2. Prediction of the drying of a cellulose acetate−acetone coating in a single-zone oven under high airflow. The oven temperature is 70 °C, and the heat-transfer coefficients are both 1.5×10^{-3} W/(cm^2 K).

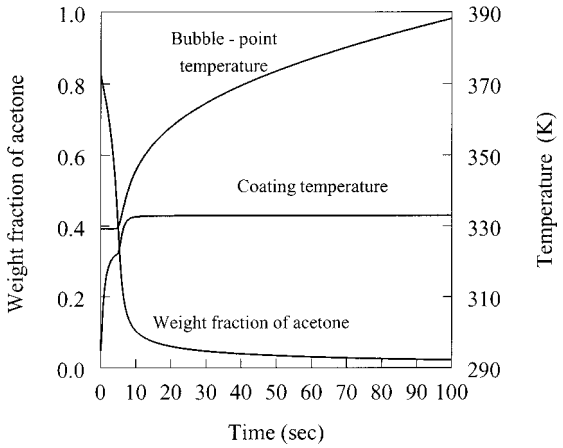

Figure 3. Prediction of the drying of a cellulose acetate−acetone coating in a single-zone oven under high airflow. The oven temperature is 60 °C, and the heat-transfer coefficients are both 1.5×10^{-3} W/(cm^2 K).

present in the coating. Figure 1 shows that, under gentle drying conditions, the coating temperature remains well below the bubble-point temperature, so no bubbles are predicted to form. To achieve lower residual acetone levels, both heat-transfer coefficients are increased from 6×10^{-4} to 1.5×10^{-3} W/(cm^2 K), while the air temperatures are kept the same. As shown in Figure 2, under these conditions, the coating temperature increases very rapidly without showing a minimum because the energy supplied by the oven air exceeds the energy consumption by evaporation. Also, at this high airflow, the acetone concentration decreases much more rapidly, and the residual acetone at the end of 100 s is predicted to be 0.73 wt %, much lower than the amount left in the coating dried under the lower airflow. However, because of the fast temperature increase at these high heat-transfer rates, the predictions have shown that bubble formation starts at the substrate−coating interface. To eliminate the dryer-induced bubbles, the solvent composition and the dryer temperature must be controlled so that boiling does not occur. If the air temperature is lowered by 10 °C, it is predicted that the coating temperature does not exceed the bubble-point temperature; however, the residual acetone level at the end of drying increases to 2.18%, as shown in Figure 3. The last two predictions illustrate the trade-off between two objectives: obtaining a defect-free coating and minimizing the residual solvent within the coating. To achieve both goals simultaneously, it is necessary to choose the appropriate dryer type and drying conditions. Figure 4 demonstrates how these objectives can be approached if the solution is dried in an oven with two zones. The drying conditions in the first zone correspond to the low-airflow case of Figure 1, whereas the conditions in the second zone are the same as those in Figure 2. Within the first 50 s under gentle drying conditions, no bubbles are predicted to form. When the coating enters the second zone, the solvent concentrations are at such levels that there is no bubble formation risk from solvent boiling. The residual acetone at the end of the second zone was predicted to be 1.36 wt % lower than the value predicted for the low-airflow case throughout the single drying zone. The effect of increasing the number of zones on the residual acetone content is shown in Figure 5. When the coating is dried in a series of eight zones instead of two zones, the weight percent of acetone at the end of

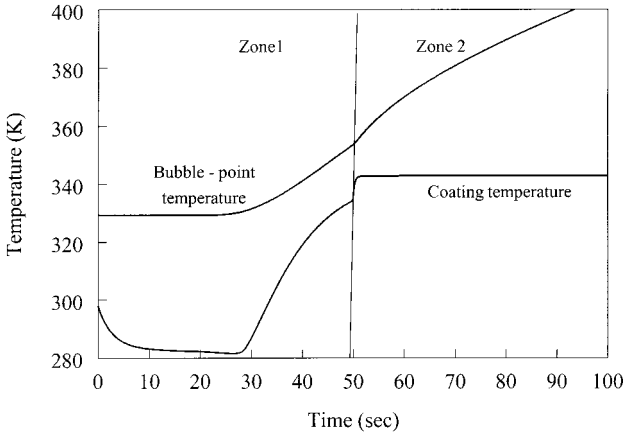

Figure 4. Prediction of the coating temperature and the bubble-point temperature at the substrate−polymer film interface for the cellulose acetate−acetone system. The air temperature in both zones is 70 °C, and the heat-transfer coefficients in zones 1 and 2 are 6×10^{-4} and 1.5×10^{-3} W/(cm^2 K), respectively.

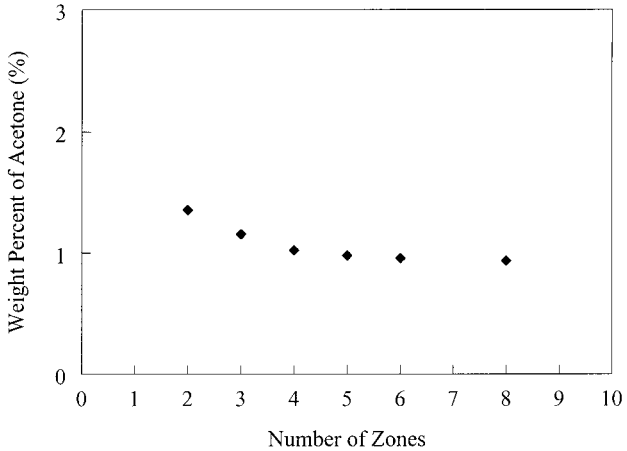

Figure 5. Prediction of the effect of the number of zones on the weight percent of acetone left in a cellulose acetate coating at the end of 100 s of drying. The air temperature in each zone is 70 °C, and the heat-transfer coefficients at the entrance of each zone are increased by equal increments from 6×10^{-4} to 1.5×10^{-3} W/(cm^2 K).

100 s of drying decreases from 1.36% to 0.94%. This is because of the strong diffusional resistance within the coating. When the heat- and mass-transfer coefficients or air temperatures are very high in the early stages of

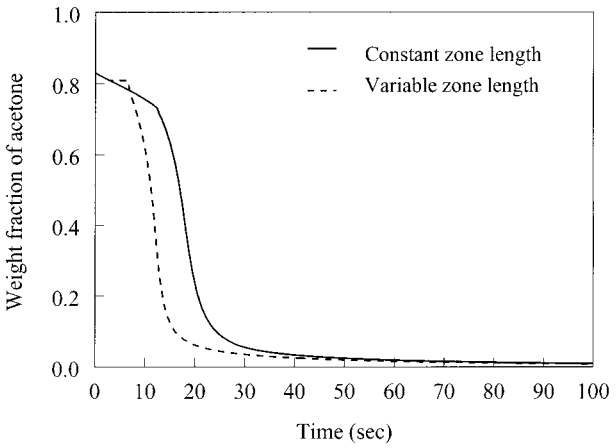

Figure 6. Prediction of the effect of variable zone length on the average weight fraction of acetone in a cellulose acetate coating. The number of zones is 8, and the air temperature in each zone is 70 °C. The heat-transfer coefficients at the entrance of each zone are increased by equal increments from 6×10^{-4} to 1.5×10^{-3} W/(cm^2 K).

drying, evaporation is so fast that the diffusivity of the solvent at the surface drops by several orders of magnitude because of its strong dependence on concentration. This phenomenon is referred to as skinning. Once the skin layer forms near the surface, diffusion of the solvent within the coating is restricted so much that it is almost impossible to remove the rest of the solvent within a reasonable period of time. When the number of zones is increased, the heat- and mass-transfer coefficients vary in a more gradual and continuous manner. Consequently, skin formation is suppressed, and at the end of the process, more solvent is removed from the coating. In multizone drying simulations, heat-transfer coefficients at the entrance of each zone were increased by equal increments from $h^g = h^G = 6 \times 10^{-4}$ W/(cm^2 °C) in the first zone to 1.5×10^{-3} W/cm^2 °C) in the last zone, while the air temperature was kept at 70 °C throughout the dryer. The values of these heat transfer coefficients correspond to oven configurations varying from mild parallel flow to impingement flow.[30] The mass-transfer coefficients were calculated using the Chilton−Coulborn analogy.[31] In previous simulations, the length of each zone was equal. However, this parameter can also be varied from zone to zone to control the residual solvent content within the coating.

Figure 6 shows the effect of a variable zone length on the weight fraction of acetone during drying in an eight-zone oven. The residence time through the ith zone, t_{Ri}, was calculated using the equation

$$t_{Ri} = t_{Ri-1}\left[1 + \alpha\left(\frac{t_D - t_i}{t_D}\right)^{\beta} t_{Ri-1}\right] \qquad (10)$$

where α and β are constants, t_i is the time at which coating enters the ith zone t_D and t_{Ri-1} are the residence times through the dryer and the previous zone $(i-1)$, respectively. The heat- and mass-transfer coefficients, air temperatures, and residence times through each zone are listed in Table 3. The residence time distribution was adjusted in such a way that the length of the zones were longer toward the end of the dryer. The benefit of such an oven configuration is more pronounced if the air temperature is also varied in each zone from $T^G = T^g = 333$ K in the first zone to 368 K in the 8th zone. In this case, the average concentration of acetone at the end of the dryer was predicted to be 0.53×10^{-5} g/cm^3, whereas the corresponding quantity was predicted to be 0.31×10^{-3} g/cm^3 at the end of an oven consisting of 8 equally spaced zones.

Table 3. Values of Dryer Parameters for Cellulose Acetate−Acetone Solution in Each Zone

zone	t_i (s)	$k_1^G \times 10^{10}$ (s/cm)	$h^G = h^g \times 10^4$ [W/(cm^2 K)]	$T^G = T^g$ (K)
1	3	8	6	343
2	6.7	35.4	26.6	343
3	11.4	62.8	47.1	343
4	17.7	90.2	67.7	343
5	26.6	118	88.3	343
6	40.2	145.8	108.9	343
7	62.6	173.2	129.4	343
8	100	200.6	150	343

Table 4. Parameters for the Polystyrene−Toluene−THF Test System Dried in a Single-Zone Oven

initial conditions	
temperature	303 K
coating thickness	0.00577 cm
initial composition of toluene	0.32 g/cm^3
initial composition of THF	0.32 g/cm^3
substrate parameters	
heat capacity	1.25 J/(g K)
density	1.37 g/cm^3
base thickness	0.003556 cm
coating parameters	
heat capacity	2.1 J/(g K)
density of polymer	1.083 g/cm^3
heat of vaporization of toluene	360 J/g
heat of vaporization of THF	435 J/g
operating conditions	
base-side heat-transfer coefficient	78×10^{-4} W/(cm^2 K)
coat-side heat-transfer coefficient	78×10^{-4} W/(cm^2 K)
bottom air supply temperature	393 K
top air supply temperature	393 K
mass-transfer coefficient of toluene	1.27×10^{-8} s/cm
mass-transfer coefficient of THF	1.1×10^{-8} s/cm

(b) Polystyrene−Toluene−Tetrahydrofuran System. In this section, the drying behavior of the polystyrene (PS)−toluene−tetrahydrofuran (THF) system was investigated. Free-volume parameters were obtained from the literature, and the Flory−Huggins interaction parameter of the PS−THF pair was predicted from a semiempirical expression.[26,32] These parameters and the other input data used in the simulation are listed in Tables 1 and 4, respectively. This system was previously simulated for a single drying zone.[7] The simulation results showed that THF evaporates very quickly because it has a higher diffusivity and higher volatility than toluene; however, its evaporation rate can be decreased by increasing its mole fraction in the gas phase. The latter result demonstrates the unique feature of the drying of multiple-solvent systems. It is possible to control the removal of the individual solvents by adjusting the solvent composition of the gas phase, and multizone oven configurations offer a great flexibility in achieving this task. Figure 7 shows the weight fractions of both solvents through a two-zone dryer. In the first zone, the mole fraction of THF is 0.3, and in the second zone, it is reduced to zero. All other operating conditions in each zone are the same as those listed in Table 4. The rates of evaporation of the two solvents in the first 7 s were predicted to be very high and then to decrease because of the strong diffusional resistance within the coating. Because there is no THF in the atmosphere in the second zone, the driving force for its evaporation is increased, and the rest of the THF in the coating is removed in that zone.

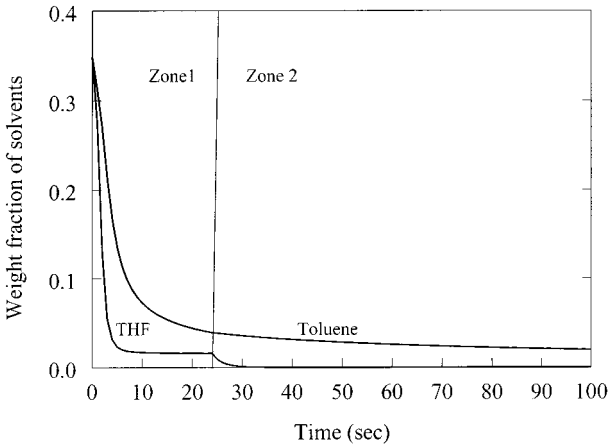

Figure 7. Prediction of the average weight fractions of solvents during drying in a two-zone oven for the PS−toluene−THF system. The air temperature and heat-transfer coefficient in both zones are 120 °C and 78 × 10^{-4} W/(cm^2 K), respectively.

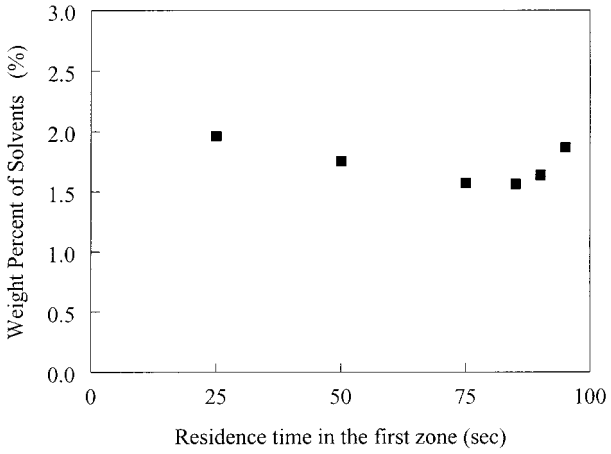

Figure 8. Prediction of the effect of zone length on the residual solvent levels for the PS−toluene−THF system at the end of 100 s of drying in a two-zone oven. The air temperature and the heat-transfer coefficient in each zone are 120 °C and 78 × 10^{-4} W/(cm^2 K), respectively.

Figure 8 shows the effect of the length of the first zone on the total residual solvent content at the end of 100 s of drying. It was predicted that the weight percent of solvent decreases when the residence time in the first zone is increased from 25 to 85 s. Under these drying conditions, if the coating remains for 85 s in the first zone, then the minimum value of the total residual solvent content is obtained. This result is again a consequence of strong diffusional resistance within the coating. By increasing the length of the first zone, the rate of evaporation of THF is kept at low values for a longer period of time, resulting in higher concentrations of THF in the coating. Because each of the solvents adds free volume to the polymer film, the higher THF concentration enhances the removal of toluene. If the residence time in the first zone is above 85 s, then there is not enough time in the second zone to remove more THF. As a result, the total residual solvent content starts to increase because of the higher THF concentration left in the coating.

In the final section, the model is evaluated by comparison with one set of experimental data collected for the polyvinyl−acetate toluene system.[33] The weight loss of the solvent is measured with an Ohaus moisture determination balance. The temperature-programmed

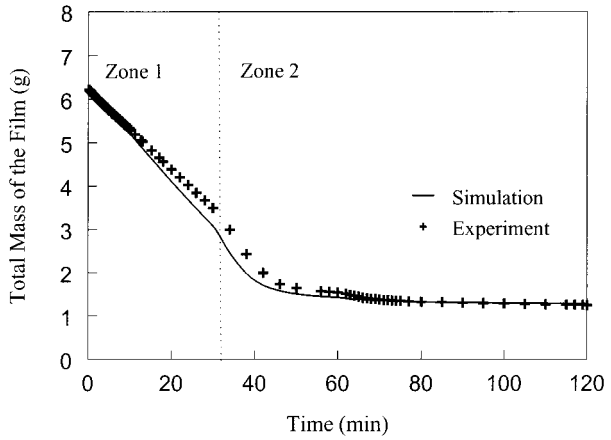

Figure 9. Comparison of experimental and simulated results for the total weight of the film as a function of time for the PVAC−toluene system dried at three different temperatures.

option of the balance allowed the sample to be dried at three different oven temperatures, 40, 60, and 80 °C. The initial thickness of the sample was 0.075 cm, and the initial weight fraction of toluene was 0.81. The experimentally determined mass-transfer coefficients at each temperature are 0.42 × 10^{-9}, 0.48 × 10^{-9}, and 0.56 × 10^{-9} s/cm, respectively. The free-volume parameters and binary interaction parameters are listed in Table 1.[26] As shown in Figure 9, the model predicts the initial drying rate, as well as the final residual amount of toluene, accurately.

Conclusion

This study has demonstrated the benefits of using multizone ovens to obtain better product quality. To analyze the drying behavior of polymer−solvent coatings in such an oven configuration, a detailed model is necessary. The drying model briefly presented here can be applied to a large number of important drying processes including drying in multiple-zone ovens. The prediction results found here have clearly shown that multizone ovens can be used to reduce the residual solvent content by controlling the vapor-phase composition, air temperature, and air velocity in each zone. Additionally, by varying these operating conditions in a more gradual and continuous manner at the entrance of each zone, it was predicted that bubble formation due to solvent boiling can be eliminated without lowering the process speeed. Furthermore, it was found that the length of the zones in an oven is an important design parameter and should be optimized based on the choice of the coating solvent. To perform such an optimization, the model presented here has the potential to serve as a tool. It can also be used as a guide for optimizing the operating conditions in existing industrial dryers.

In this study, the validity of only the binary model in predicting the drying process in multiple-zone oven configurations was confirmed by using one set of experimental data. However, more experimental results are needed to evaluate the multicomponent drying model.

Acknowledgment

I thank Prof. J. Larry Duda of the Center for Polymer−Solvent Studies at the Pennsylvania State University for his valuable discussion and advice.

Literature Cited

Cairncross, R. A.; Price, P. E.; Francis, L. F.; Scriven, L. E. Skinning Phenomena in Drying Coatings: An Assessment. AIChE Spring National Meeting, Atlanta, GA, April 1994.

Cairncross, R. A.; Jeyadev, R.; Dunham, R. F.; Evans, K.; Francis, L. F.; Scriven, L. E. Modeling and Design of an Industrial Dryer With Convective and Radiant Heating. *J. Appl. Polym. Sci.* **1995**, *58*, 1279.

Alsoy, S.; Duda, J. L. Drying of Solvent Coated Polymer Films. *Drying Technol.* **1998**, *16*, 15.

Vrentas, J. S.; Duda, J. L. Diffusion in Polymer−Solvent Systems II. A Predictive Theory for the Dependence of Diffusion Coefficients on Temperature, Concentration and Molecular Weight. *J. Polym. Sci.* **1977**, *15*, 417.

Vrentas, J. S.; Duda, J. L. Solvent and Temperature Effects on Diffusion in Polymer−Solvent Systems. *J. Appl. Polym. Sci.* **1977**, *21*, 1715.

Vrentas, J. S.; Duda, J. L. Molecular Diffusion in Polymer Solutions. *AIChE J.* **1979**, *25*, 1.

Alsoy, S.; Duda, J. L. Modeling of Multicomponent Drying of Polymer Films. *AIChE J.* **1999**, *45*, 896.

Cohen, E.; Gutoff, E. *Modern Coating and Drying Technology*; VCH Publishers: New York, 1992.

Hansen, C. M. A Mathematical Description of Film Drying By Solvent Evaporation. *J. Oil Colour Chem. Assoc.* **1968**, *51*, 27.

Okazaki, M.; Shioda, K.; Masuda, K.; Toei, R. Drying Mechanism of Coated Film of Polymer Solution. *J. Chem. Eng. Jpn.* **1974**, *7*, 99.

Blandin, H. P.; David, J. C.; Vergnaud, J. M. Modeling of Drying of Coatings: Effect of the Thickness, Temperature and Concentration of Solvent. *Prog. Org. Coat.* **1987**, *15*, 163.

Blandin, H. P.; David, J. C.; Vergnaud, J. M.; Illien, J. P.; Malizewicz, M. Modeling the Drying Processes of Coatings With Various Layers. *J. Coat. Technol.* ***1987***, *59*, 27.

Yapel, R. A. A Physical Model of the Drying of Coated Films. M.S. Thesis, University of Minnesota, Minneapolis, MN, 1988.

Waggoner, R. A.; Blum, D. F. Solvent Diffusion and Drying of Coatings. *J. Coat. Technol.* **1989**, *61*, 51.

Vrentas, J. S.; Vrentas, C. M. Drying of Solvent Coated Polymer Films. *J. Polym. Sci. B: Polym. Phys.* **1994**, *32*, 187.

Gutoff E. B. Modeling Solvent Drying of Coated Webs Including the Initial Transient. *Drying Technol.* **1996**, *14*, 1673.

Duda, J. L.; Vrentas, J. S.; Ju, S. T.; Liu, H. T. Prediction of Diffusion Coefficients for Polymer Solvent Systems. *AIChE J.* **1982**, *28*, 285.

Vrentas, J. S.; Duda, J. L.; Ling, H. C.; Hou, A. C. Free Volume Theories for Self-Diffusion in Polymer Solvent Systems. II. Predictive Capabilities. *J. Polym. Phys.* **1985**, *23*, 289.

Vrentas, J. S.; Chu, C. H. Predictive Capabilities of a Free Volume Theory for Solvent Self-Diffusion Coefficients. *J. Polym. Sci B: Polym. Phys.* **1989**, *27*, 1179.

Bearman, R. J. On the Molecular Basis of Some Current Theories of Diffusion. *J. Phys. Chem.* **1961**, *65*, 1961.

Vrentas, J. S.; Duda, J. L.; Hou, A. C. Enhancement of Impurity Removal from Polymer Films. *J. Appl. Polym. Sci.*, **1985**, *30*, 4499.

Zielinski, J. M.; Hanley, B. F. Practical Friction-Based Approach to Modeling Multicomponent Diffusion. *AIChE J.* **1999**, *45*, 1.

Vrentas, J. S.; Duda, J. L.; Ling, H. C. Self-Diffusion in Polymer−Solvent Systems. *J. Polym. Sci.* **1984**, *22*, 459.

Flory, P. J. *Principles of Polymer Chemistry*; Cornell University Press: Ithaca, NY, 1953.

Favre, E.; Nguyen, Q. T.; Clement, R.; Neel, J. Application of Flory−Huggins Theory To Ternary Polymer−Solvents Equilibria: A Case Study. *Eur. Polym. J.* **1996**, *32*, 303.

Zielinski, J. M.; Duda, J. L. Predicting Polymer/Solvent Diffusion Coefficients Using Free Volume Theory. *AIChE J.* **1992**, *38*, 405.

Dabral, M.; Francis, L. F.; Scriven, L. E. Structure Evolution in Asymmetric Polymer Coatings. 9th International Coating Science and Technology Symposium, Newark, NJ, May 1998.

Anderson, J. E.; Ullman, R. Mathematical Analysis of Factors Influencing the skin Thickness of Asymmetric Reverse Osmosis Membranes. *J. Appl. Phys.* **1973**, *44*, 4303.

Reid, R. C.; Prausnitz, J. M.; Poling, B. E. *The Properties of Gases and Liquids*; McGraw-Hill: New York, 1987.

Price, P. E.; Cairncross, R. A. Optimization of Single Zone Drying of Polymer Solution Coatings Using Mathematical Modeling. *J. Appl. Polym. Sci.* **2000**, *78*, 149.

Incropera, F. P.; De Witt, D. P. *Fundamentals of Heat and Mass Transfer*; John Wiley and Sons: New York, 1990.

Bristow, G. M.; Watson, W. F. Cohesive Energy Densities of Polymers: 1. Cohesive Energy Densities of Rubbers by Swelling Measurements. *Trans. Faraday Soc.* **1958**, *59*, 27.

Alsoy, S. Modeling of Polymer Drying and Devolatilization Processes. Ph.D. Thesis, The Pennsylvania State University, University Park, PA, 1998.

Received for review August 15, 2000
Revised manuscript received March 8, 2001
Accepted March 9, 2001

IE000751+